Vibrations of Complete Spherical Shells With Imperfections

Article *in* Journal of Vibration and Acoustics · June 2007

DOI: 10.1115/1.2731415

4 authors, including:

Amy Robertson
National Renewable Energy Laboratory
86 PUBLICATIONS **2,555** CITATIONS
SEE PROFILE

Michael Steinzig
Los Alamos National Laboratory
32 PUBLICATIONS **718** CITATIONS
SEE PROFILE

Vibrations of Complete Spherical Shells With Imperfections

Thomas A. Duffey
Consulting Engineer
PO Box 1239
Tijeras, NM 87059

Jason E. Pepin
Technical Staff Member
Los Alamos National Laboratory
Los Alamos, NM 87545

Amy N. Robertson
Consulting Engineer
Hytec, Inc.
4735 Walnut, Suite W-100
Boulder, CO 80305

Michael L. Steinzig
Chief Engineer – Optical Imaging
Hytec, Inc.
110 Eastgate Drive
Los Alamos, NM 87544

ABSTRACT

Numerous theoretical investigations on the natural frequencies for complete spherical shells have been reported over the past four decades. However, attempts at correlating the theoretical results with either experimental or simulated results (both for axisymmetric and non-axisymmetric modes of vibration) are almost completely lacking. In this paper, natural frequencies and mode shapes obtained from axisymmetric and non-axisymmetric theories of vibration of complete spherical shells and from Finite Element computer simulations of the vibrations, with and without geometrical imperfections, are presented. Modal tests reported elsewhere on commercially available, thin spherical marine floats (with imperfections) are utilized as a basis for comparison of frequencies to both the theoretical and numerical results. In addition, results of a 'whole field' measurement on one of the imperfect shells using dynamic holography are presented. Because of the imperfections present, 'splitting' of frequencies of non-axisymmetric modes is anticipated. Correlations of recorded natural frequencies of the spherical shells with earlier theoretical results and with finite element simulations for the first few modes are good, and the presence of the frequency splitting phenomenon is demonstrated.

1. INTRODUCTION

The modal response of complete spherical shells (see Fig 1) has been investigated with progressively higher-order theories since the 1960's. While the emphasis has been on the axisymmetric modes of vibration [1-3], theoretical investigations regarding the non-axisymmetric modes have been reported as well [4-6]. The axisymmetric modes are independent of the circumferential coordinate, whereas the non-axisymmetric modes depend upon both meridional and circumferential coordinates, but are degenerate for a complete, perfect spherical shell.

The first to examine axisymmetric modes of a complete spherical shell were Baker [1] and Kalnins [2], who used membrane and elementary bending theories, respectively. These axisymmetric modes are independent of the circumferential angle, θ (See Fig. 1). Modes of vibration are expressed in terms of Legendre Polynomials of integer indices, n. For each value of $n \geq 2$, there are two branches, i.e., two separate, but similar, mode shapes, and two distinct frequencies (for n = 0, there is only one real root, corresponding to the 'fundamental' membrane or 'breathing' mode). The frequency spectrum therefore consists of two infinite sets of modes. Kalnins [2] labeled one branch as flexural and the other as membrane, the distinction made on the basis of the comparison of strain energies due to bending and stretching of each mode. Wilkinson [3] subsequently investigated the axisymmetric

modes of a complete spherical shell, but included the effects of transverse shear and rotary inertia as well. His

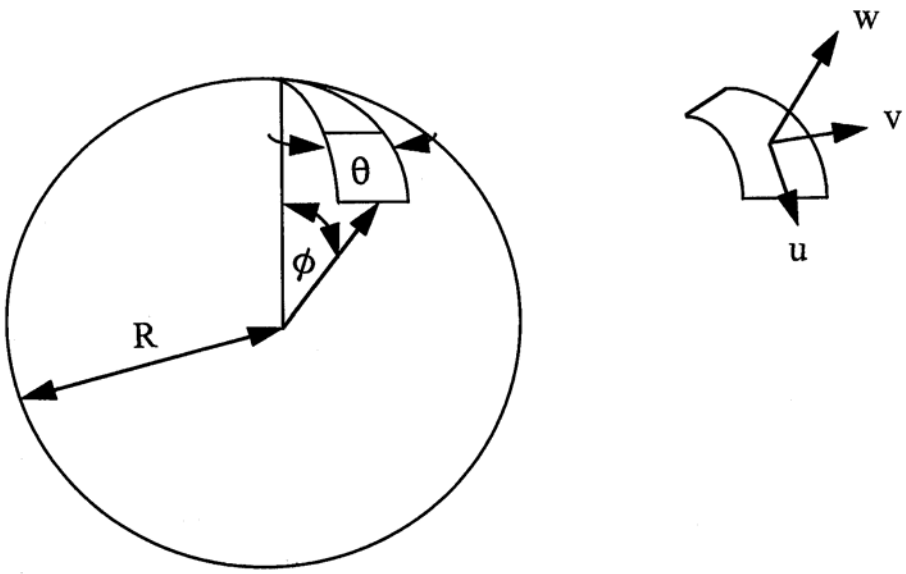

Figure 1. Complete Spherical Shell

investigation resulted in the identification of a third, higher modal branch, although the two lower branches were nominally identical to those of Kalnins [2].

Silbiger [4] presents the first discussion of the presence of nonaxisymmetric modes of spherical shells. These nonaxisymmetric modes depend upon both θ and ϕ (See Fig. 1). Silbiger [4] claims that nonaxisymmetric modes for a complete spherical shell do exist and that they are degenerate, meaning that the nonaxisymmetric frequencies are identical to corresponding axisymmetric modes. Silbiger [4] attributes this to the spherical symmetry of the shell. He argues that the axisymmetric modes are defined with respect to a specific set of axes. Due to the symmetry of the shell, however, it can vibrate in similar modes with a different axis orientation. For a given set of 'identical' modes (differing only in orientation), the modes will each have the same natural frequency. These axisymmetric modes of identical natural frequency can be superimposed to obtain new non-axisymmetric modes that have the same natural frequency as the corresponding axisymmetric mode, but which are not symmetric with respect to any axis. Silbiger [4] goes on to state that, corresponding to each natural frequency, there exist 2n+1 linearly independent modes. All other modes (at a given frequency) are linear combinations of these modes. However, he observes that when a deviation from spherical symmetry occurs, this degeneracy disappears and the modes will split into 2n+1 distinct frequencies.

Niordson [5] rederived the equations for bending vibrations of a spherical shell in a somewhat different form. He examined the non-axisymmetric modes as well, concluding that there exist n+1 (not 2n+1 as reported by Silbiger) modes at each mode number, n, on each branch. Observations in [5] made regarding non-axisymmetric modes (e.g., the fact that they exhibit the frequency degeneracy identified by Silbiger [4]) were similar, except for the number of independent modes anticipated. In a later paper, Niordson [6] similarly indicates that when spherical symmetry of a complete spherical shell is lost, the previously degenerate frequencies form into bands, with the bandwidth related to the degree of spherical asymmetry.

With the exception of Baker's [1] work on spherical shells (using membrane theory) and some very limited comparisons by Duffey and Romero [7] on spherical vessels with massive nozzles, the authors are unaware of any attempts at correlation of theoretical predictions of natural frequencies of complete spherical shells with experimental data. Moreover, the splitting of the degenerate non-axisymmetric modes of vibration in the case of perturbations from ideal spherical shell geometry has only been postulated. It has not been demonstrated experimentally for a free, complete spherical shell. A detailed literature review and interpretation of axisymmetric and non-axisymmetric vibrations for both perfect and imperfect spherical shells is presented in [7]. Splitting of

degenerate modal frequencies has recently been exploited in [8] for characterizing non-uniformities in precision symmetric parts and has been applied to hemispherical shells.

In this paper, a series of modal tests reported in [9] on commercially available, stainless steel, spherically shaped, thin-wall marine floats are utilized as a basis for comparison of frequencies to both theoretical and numerically calculated frequencies. In addition, comparisons with PRISM (Precision Real-Time Instrument for Surface Measurement) 'whole field' measurements on one of the spherical shells using dynamic holography are presented [10]. The floats are complete spherical shells, but contain imperfections [11]. Natural frequencies obtained are compared with axisymmetric and non-axisymmetric theories of vibration of complete spherical shells. In addition, comparisons are made to finite element modal calculations that include measured variations in both radius and shell thickness.

In Section 2, axisymmetric modes are investigated. Correlations of averaged natural frequencies for the entire set of spherical shells with earlier axisymmetric theoretical results [3] for the first few modes are presented. In Section 3, non-axisymmetric modes are investigated. Using the PRISM Method for one particular shell and accelerometer measurements recorded earlier on the same shell, the presence of the frequency splitting phenomenon associated with the non-axisymmetric modes is investigated for the imperfect spherical shell. Average thickness and radius profile measurements as a function of the meridional coordinate are then utilized used as input in the Finite Element Model for further investigation of frequency splitting. Comparisons of results are presented in Section 4 and conclusions are drawn in Section 5.

2. AXISYMMETRIC MODES OF VIBRATION

2.1 Theoretical Frequencies and Mode Shapes

The modal frequencies for a thin spherical shell are given by

$$f_i = \frac{\lambda_i}{2\pi R}\left[\frac{E}{\mu\left(1-\nu^2\right)}\right]^{1/2} \tag{1}$$

where f_i is the frequency in Hertz, R is the mid-surface radius, μ is the density, E is the modulus of elasticity, and ν is the Poisson's ratio. The parameter λ_i in Equation 1 takes on a variety of forms depending upon the level of the shell theory utilized. For a higher order shell theory, including the effects of bending (these formulae include transverse shear and rotary inertia as well). Wilkinson [3] reports the natural frequencies of the nontorsional axisymmetric modes as given by the roots of the following cubic equation in λ^2:

$$\alpha\lambda^6 - \beta\lambda^4 + \delta\lambda^2 - \gamma = 0$$

where

$$\alpha = 2k_s k_1 (k_r k_1 - c_r c_1)/(1-\nu)$$

$$\beta = (k_r k_1 - c_r c_1)\left[r + 4k_s(1+\nu)/(1-\nu)\right]$$
$$+ k_1\left[\xi(k_1 + c_1) + c_r + k_r + 2k_s(k_1 + k_r)(r/(1-\nu) - 1)\right] \tag{2}$$

$$\delta = (\xi c_1 + c_r)(1+\nu)(2-r) + k_r[r(r-3-\nu) + 2(1+\nu)$$
$$\mathrm{X}((r-2)k_s + 1)] + k_1[2k_s r(r+4\nu)/(1-\nu) + r(r+\xi+\nu) + (1+3\nu)(\xi - 2k_s) - (1-\nu)]$$

and

$$\gamma = (r-2)[r(r-2) + 2k_s(1+\nu)(r-1+\nu) + (1-\nu^2)(\xi+1)]$$

The following definitions apply:

$$\lambda = \omega R[(1-\nu^2)\mu/E]^{1/2}$$
$$k = \frac{h^2}{12R^2}$$
$$\xi = \frac{1}{k}$$
$$k_1 = 1 + k$$
$$k_r = 1 + 1.8k \qquad (3)$$
$$c_1 = 2k$$
$$c_r = 2$$
$$k_s \approx 1.2$$
$$r = i(i+1)$$
$$h = \text{shell thickness}$$

The above equations were evaluated for the following nominal or averaged geometrical and material properties of the thin, spherical shells discussed above. The averaging process facilitates comparison with axisymmetric modes, as the data are similarly averaged.

Poisson's Ratio, ν = 0.28
Radius, R = 4.4688 in
Elastic Modulus, E = 28.0 X 10^6 psi
Mass Density, μ = 0.000751 lbf-sec^2/in^4
Thickness, h = 0.0625 in

A plot of natural frequencies for the higher order theory given in Eqns. 1-3 is shown in Fig. 2. Equation 1 also includes the effects of transverse shear and rotary inertia, which introduces a much higher branch (not shown in Fig. 2), which is of little interest in the present study. The floats are well into the "thin shell" region, with a radius-to-thickness ratio of 71.5. For thicker shells, e.g., the study in [7], the differences between the "bending" branches for the membrane and higher order theories become more pronounced. Inspection of Fig. 2 reveals that there is a point where frequencies on the lower branch for higher model index, n, are larger than upper branch frequencies for small n. It is interesting to note that n = 0 on the membrane branch is the so-called "fundamental", pure breathing, mode of the spherical vessel. Therefore, there are frequencies, composed largely of bending, that lie below the "fundamental" mode.

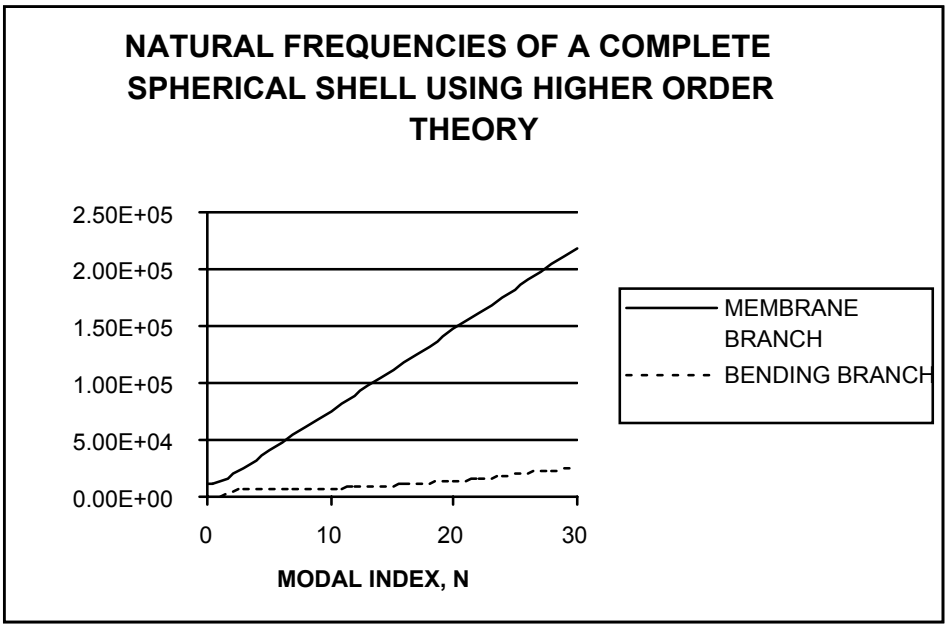

Figure 2. Float Frequencies using Higher Order Theory

As an illustration of the axisymmetric mode shapes, the first three (n = 2, 3, and 4) modes on the lower branch are shown in Figure 3. Torsional modes are not expected to be significantly excited during testing, and are not considered in this study.

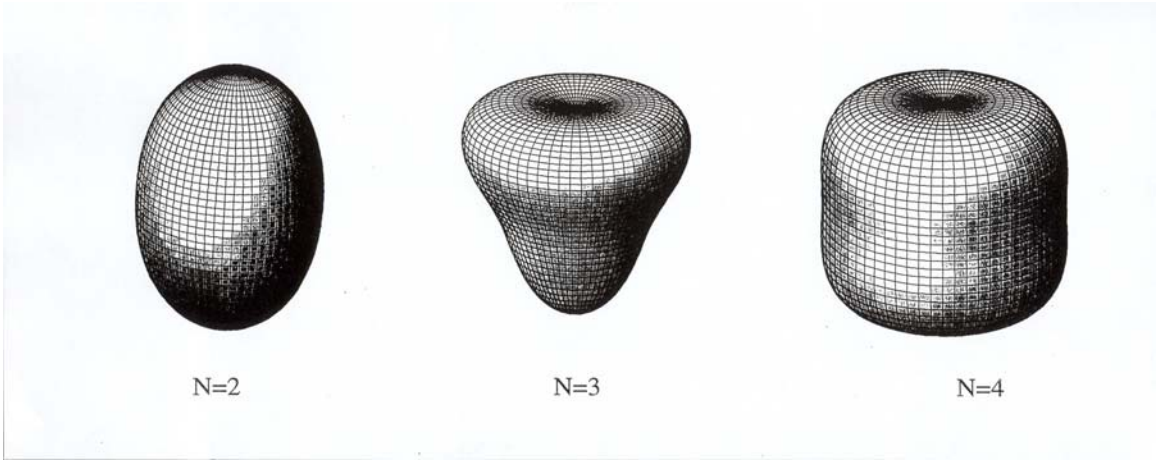

Figure 3. First Three Lower Branch Axisymmetric Modes of a Complete Spherical Shell

2.2 Comparison of Axisymmetric Modal Frequencies with Experiments

Robertson, et al [9] performed a series of modal experiments on a set of hollow, almost spherical marine floats. From the recorded FRF data, an Eigen-system Realization Algorithm (ERA) Fit was performed to determine the natural frequencies of the first four modes. Testing was performed on multiple floats. The modal values listed in Table 1 correspond to the “unit-to-unit” averaged modal frequency values reported in [9].

This averaging process effectively cancels out modal splitting and associated non-axisymmetric modes. Results can therefore be directly compared with axisymmetric theoretical results, as shown in Table 1. It can be seen that agreement between analytical (Eqn. 1) and experimental results are well within 1-percent for the first four detected modes. These differences can be attributed to variations in geometry described above. Note that the experimental frequencies are compared to those of a perfect spherical shell. The frequencies lie on the lower (primarily bending) branch, and correspond to n=2, 3, 4, and 6, respectively. The first mode, n=1, is the rigid-body mode of zero frequency. The mode n=5 was not extracted.

Table 1: Comparison of Averaged Modal Results [9] with Axisymmetric Theory

Mode	Mean Exp.	Analytical	Percent Difference
n=2, LOWER	5088	5078	0.20
n=3, LOWER	6028	6005	0.38
n=4, LOWER	6379	6378	0.02
n=6, LOWER	6680	6729	0.73

3. NON-AXISYMMETRIC MODES OF VIBRATION

An example of degenerate, non-axisymmetric modes (n=5, lower branch) for a perfect spherical shell is shown in Figure 4. Note that there are 2n+1 = 11 mode shapes in this case, one axisymmetric and ten non-axisymmetric, all with the same natural frequency.

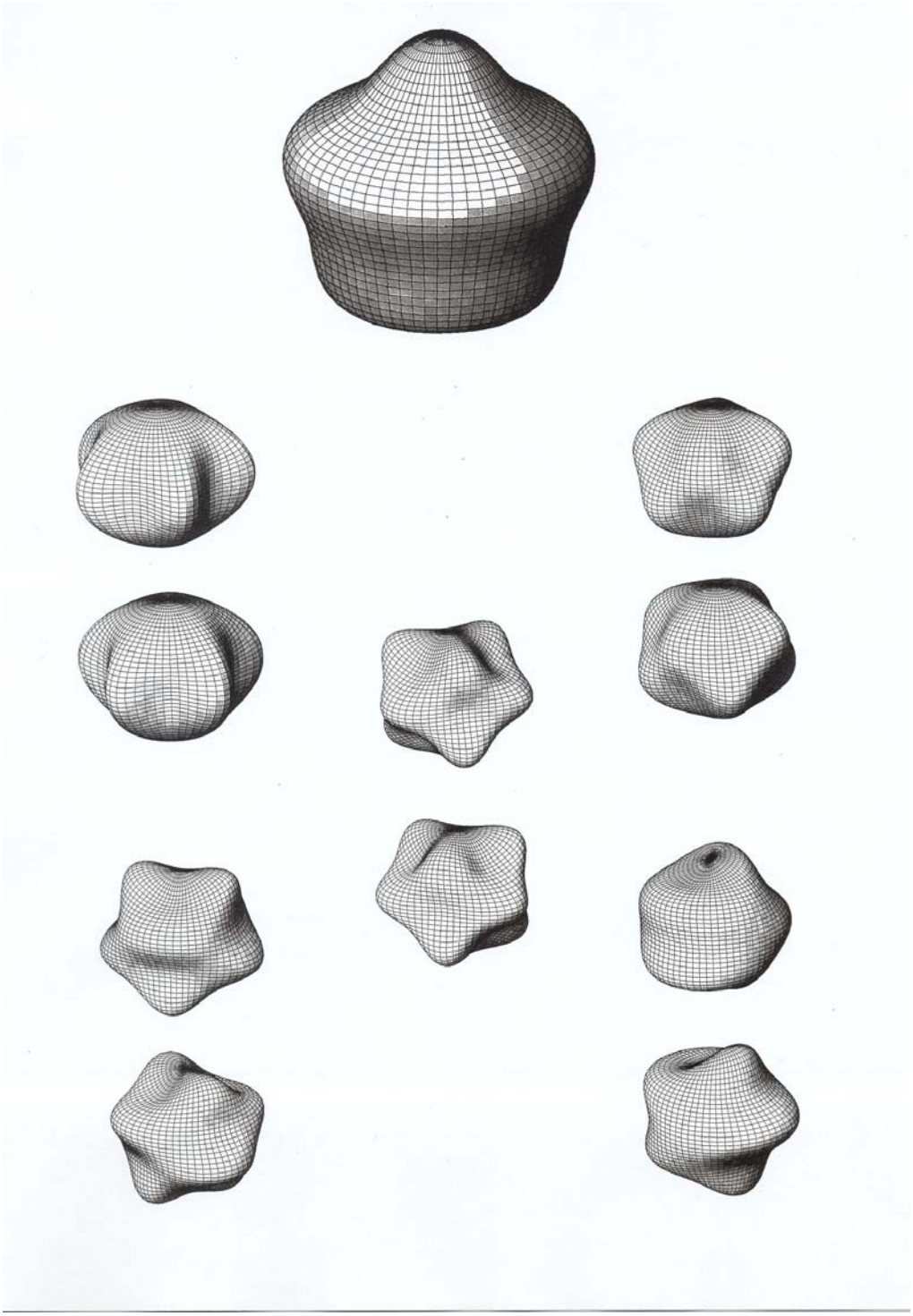

Figure 4. Degenerate Non-Axisymmetric Modes for n = 5

As discussed above, the spherical shells tested in [9, 11] contain both geometrical and material imperfections. Because of the low level of excitation in the modal tests performed on the shells, material imperfections will play little role, as the elastic properties will vary little within a given shell, and from shell to shell. However, variations in geometry (i.e, thickness and radius) could potentially be significant, as they could trigger the splitting of modal frequencies discussed above.

Results presented for axisymmetric modes of vibration in Section 2 are based upon averages over all spherical shells tested, as reported in [9]. The result is that the non-axisymmetric modes are effectively removed by the

averaging process. In order to directly observe the presence of the non-axisymmetric modes, a single marine float from the group originally tested in [9] was selected for further evaluation. This shell, No. 17, had earlier been subjected to the accelerometer modal testing during the test series described in [9], and these data were made available to the authors for the non-axisymmetric mode investigation reported herein. Also, the geometry of the shell had not been previously measured, which would involve destruction of the shell, so it was available for further investigation using the dynamic holography method described later in this paper.

In the following sub-sections, results from further investigation of the Shell No. 17 accelerometer modal data, additional testing of the same float using dynamic holography (PRISM Methodology), physical measurements performed on Shell No. 17, and finite-element modeling of this shell, are presented. Note that the FE model is based upon average meridional variations in radius and thickness using measurements of other similar shells. Considerable variation in geometry was observed from shell to shell. Measurements on shell No. 17 are currently in process, but FE results herein pertain only to average measurements for other shells. Correlations with FE results from Shell No. 17 will be compared in the future.

3.1 Accelerometer Modal Results for Float No. 17

The Eigensystem Realization Algorithm was used to convert time-domain data obtained from the authors of [9] to modal frequencies. Results are shown for one accelerometer mounted on Shell 17 in Figure 5.

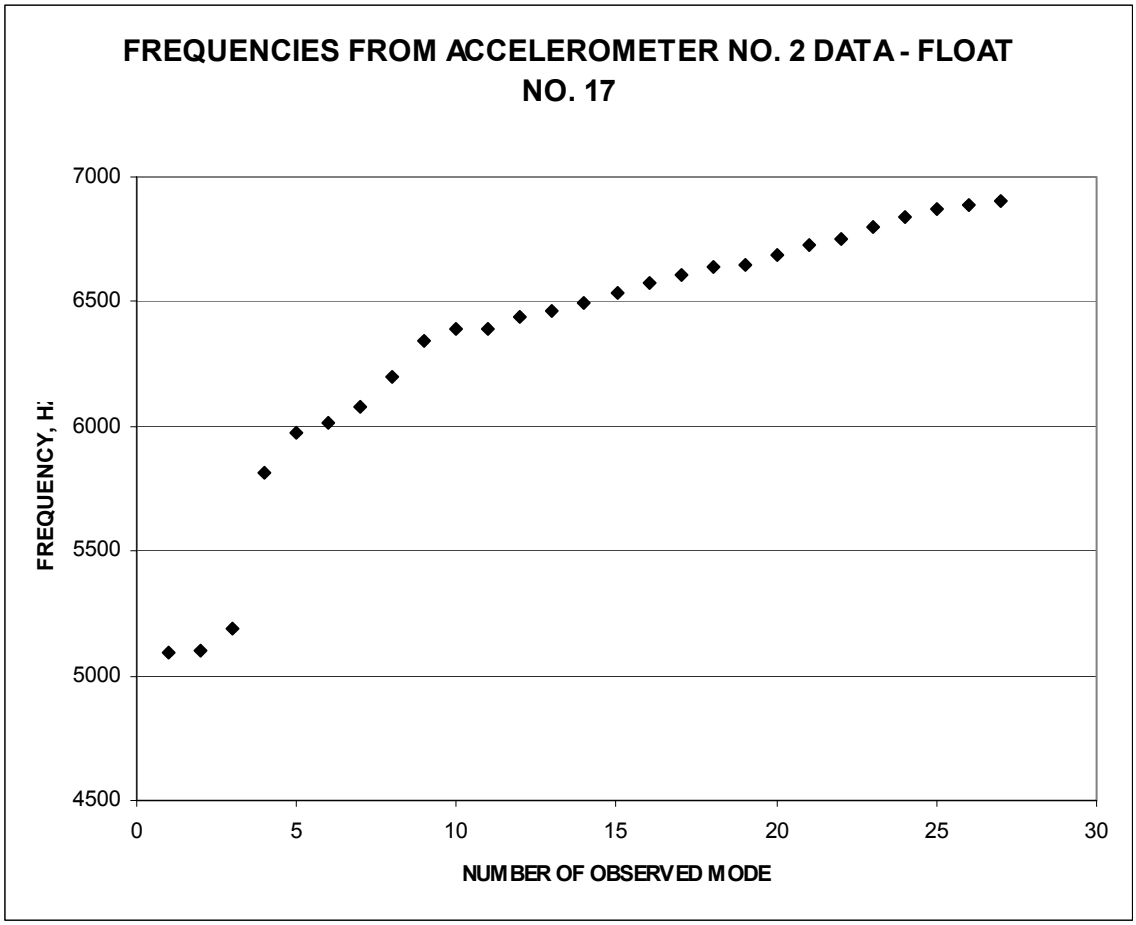

Figure 5. Frequencies from Accelerometer No. 2 Data – Float No. 17

3.2 Dynamic Holography Measurements

Whole-field vibration measurements were obtained with time-averaged holography [10], using a PRISM® system, a commercially available electronic speckle pattern interferometer. This non-contact method produces a real-time, full image of the spherical shell, with fringes indicating the mode shapes. By exciting the spherical shell with a single-frequency piezoelectric driver, a frequency sweep in the range of interest (in this case < 5000Hz to 7000 Hz) is performed, and the image of the amplified mode shape at resonance appears. Both resonant natural frequencies and associated mode shapes are therefore obtained directly.

Using this methodology on Shell No. 17 in the frequency range given above, the resonant frequencies shown in Figure 6 were obtained.

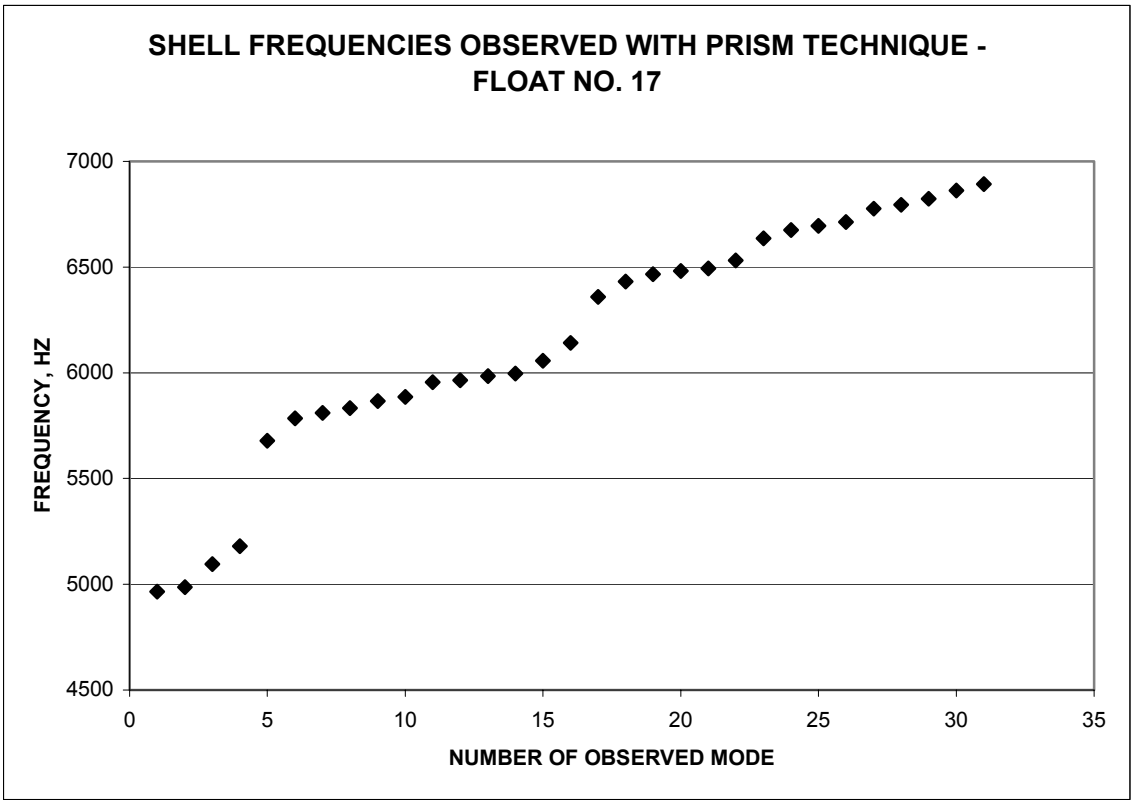

Figure 6. Resonant Frequencies Obtained on Shell No. 17 Using PRISM Whole Field Technique.

As an illustration of mode shapes obtained from this technique, images of Shell No. 17 without excitation and at an excitation frequency of 5093 Hz are shown in Figures 7 and 8, respectively. Dark fringes denote displacement normal to the plane of the image.

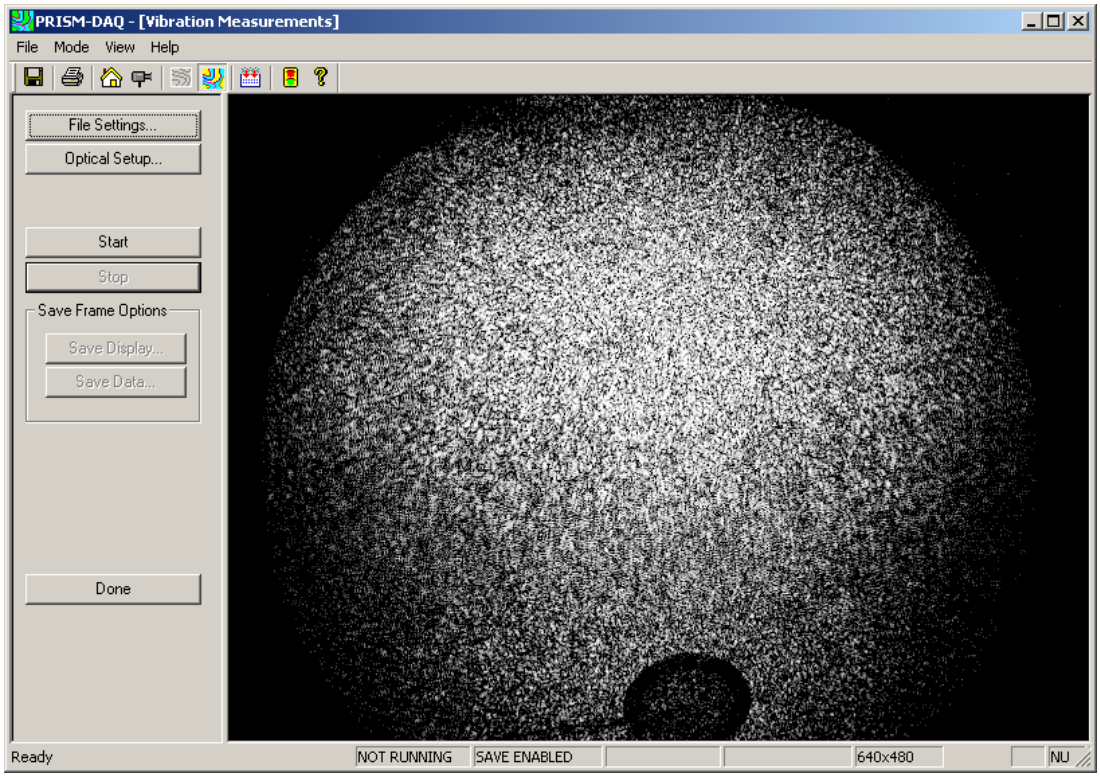

Figure 7. Shell No. 17 Before Excitation

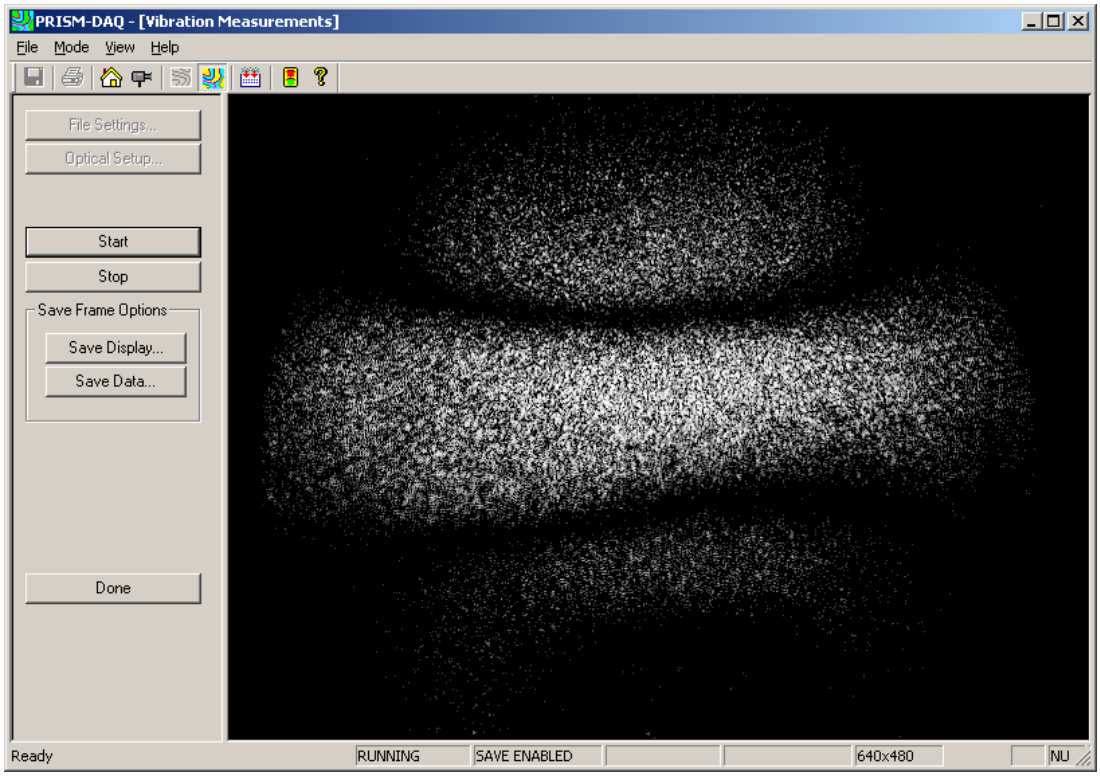

Figure 8. Float No. 17 – First Observed Mode (5093 Hz)

3.3 Planned Measurement of Variations in the Geometry of Shell No. 17

Geometric measurements of Shell 17 are underway to examine its deviation from a perfect sphere, but are incomplete at the time of writing. The measurement procedures being utilized are similar to that presented in [11], except that initial external physical measurements of the float are being taken before cutting to determine shape changes as a result of the cutting process and subsequent relief of weld residual stresses. Briefly, the shell is cut in half in a plane perpendicular to the girth weld. A coordinate measuring machine is then utilized to measure the resulting two hemispheres. Each of the hemispheres is measured along three meridians, located 45-degrees apart. These contour lines are to be measured at one-degree meridional increments, on both sides of the hemisphere. The thickness will then be determined as the distance between the inner and outer point; and the radius will be determined as the average of inner and outer points. For display purposes, each meridional contour will be divided in half, and the thickness and radius were displayed as a function of the meridional angle, with θ = 0 at the weld location and θ = 90-degrees at the pole.

3.4 Finite Element Modal Calculations

Using averaged geometric information from [11], Finite Element calculations of normal mode frequencies were performed for Float No. 17. Three cases were examined:

1. Ideal Spherical Shell – Full shell model
2. Variation in (average) thickness as a function of the meridional coordinate
3. Variation in both average thickness and average radius as a function of the meridional coordinate

The first six modes extracted for each case correspond to the three rigid-body translational and rotational degrees of freedom at zero frequency. The next five modes (7-12) are shown in Table 2 and correspond to the theoretical n=2 lower branch (See Eqn. 1). It can be seen that Case 1 is in excellent agreement with theory, and that negligible splitting occurs. Case 2 exhibits significant splitting of modal frequencies, and case 3 has significantly greater splitting, as expected.

Table 2 N=2 Lower Branch Results

Theory	Mode No.	FE 1	FE 2	FE 3
5078	7	5079.7	5058.0	4911.3
5078	8	5079.9	5058.7	4911.8
5078	9	5079.9	5072.2	5025.7
5078	10	5080.0	5078.7	5054.4
5078	11	5080.1	5079.2	5055.1

All modes extracted up to 6900 Hz are shown for the three cases in Figs. 9-11, respectively. Again, it is emphasized that geometric measurements were based upon average variations from other shells, and that future work will include measurement of thickness and radius variations for Shell No. 17.

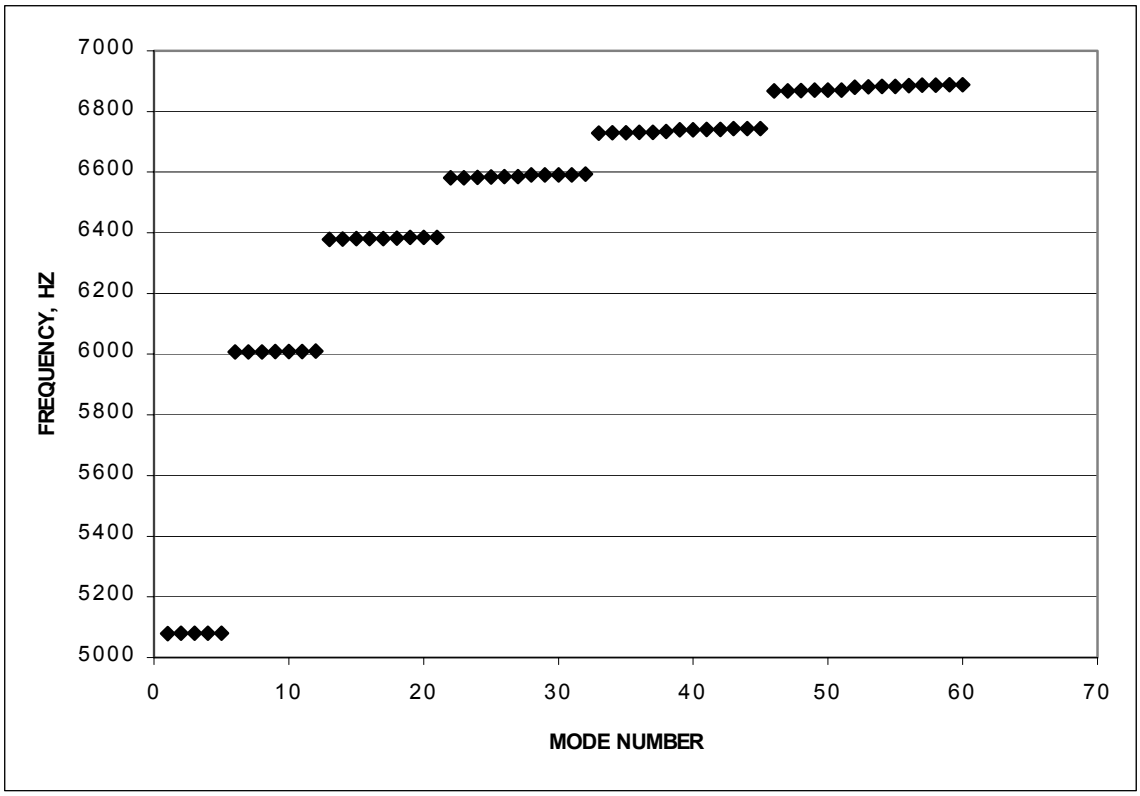

Figure 9. Finite Element Simulations for Nominal Thickness and Radius

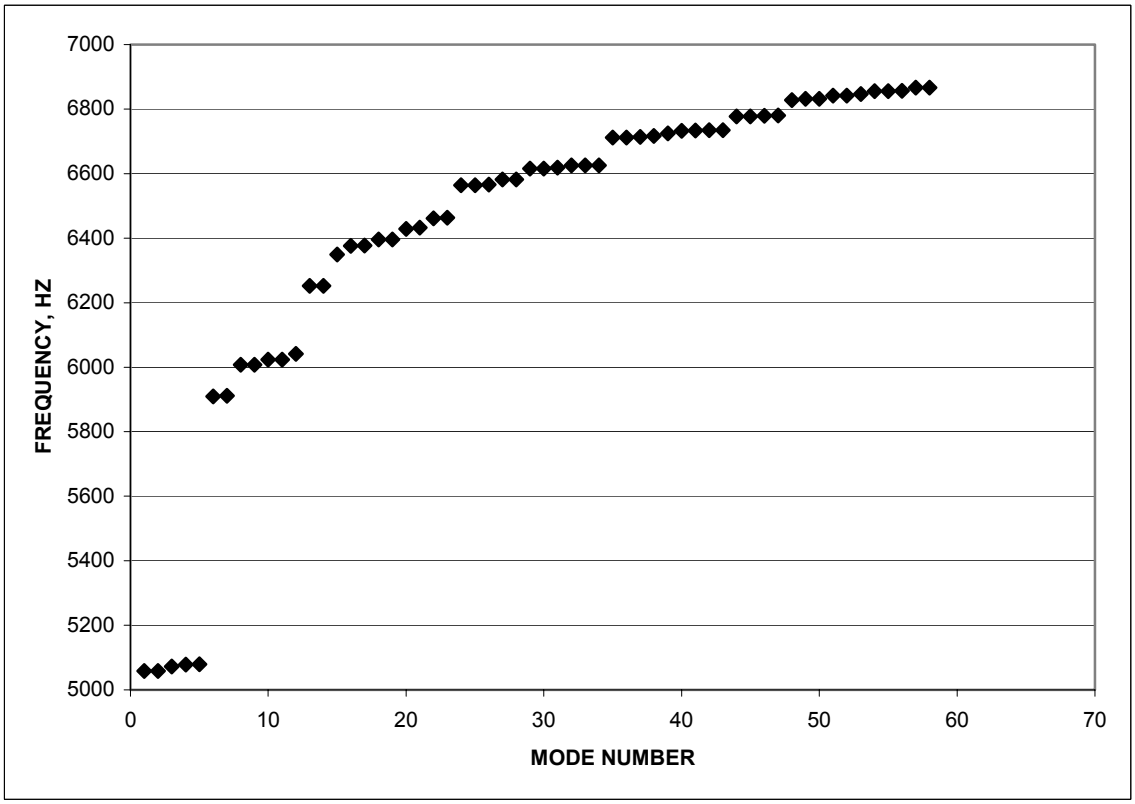

Figure 10. Finite Element Simulations Including Meridional Variations in Thickness

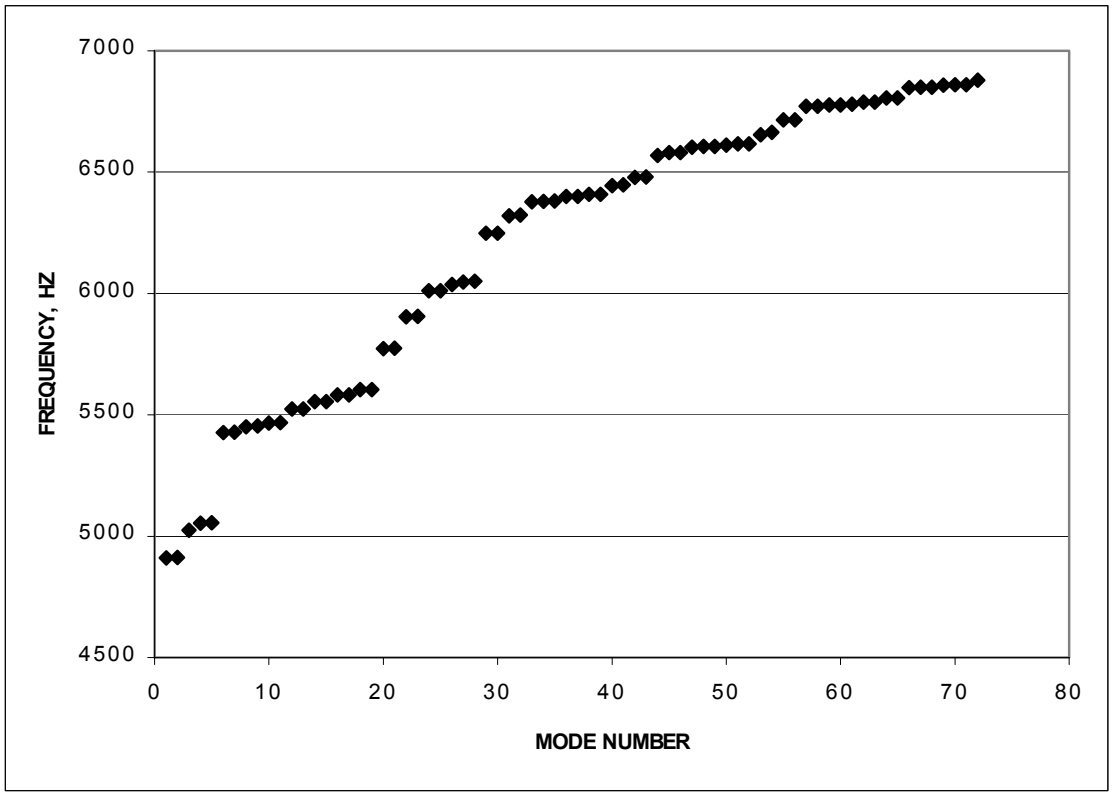

Figure 11. Finite Element Simulations Including Meridional Variations in Both Radius and Thickness

4. COMPARISONS OF RESULTS

Comparisons of the results specific to spherical shell No. 17 for n = 2 are shown in Fig. 12, where it is seen that excellent agreement is found between the PRISM whole-field method and the ERA results from the Accelerometer records. FEM calculations are based upon averaged spherical shell geometry, so the differences for the FEM calculations would be anticipated. Measurements on spherical shell No. 17 currently are being performed so that FEM calculations specific to that shell can be performed and compared to PRISM and Accelerometer results.

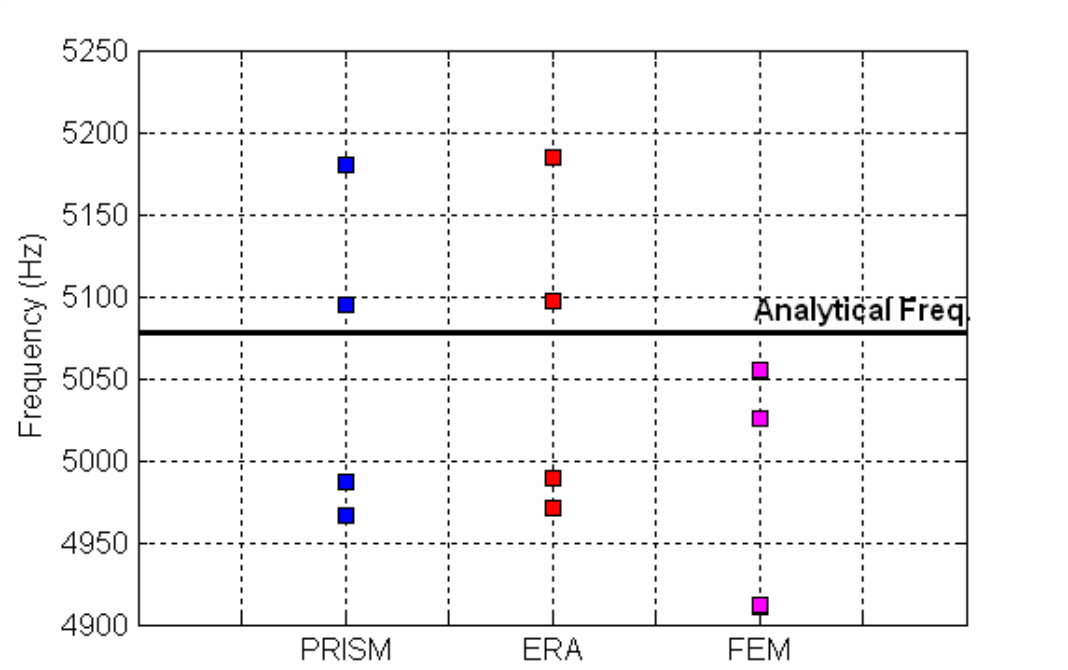

Figure 12. Comparison of extracted modal frequencies from ERA, PRISM, and FEM, n=2

5. CONCLUSIONS

Correlations of recorded natural frequencies of complete, free spherical shells are performed with both theoretical results and finite element simulations. Comparisons of the first few axisymmetric modes are good. An investigation of the non-axisymmetric modes for the case of an imperfect spherical shell reveals the presence of these non-axisymmetric modes because of the observed frequency splitting. Limited results on mode shape are presented, both from calculations and from the whole-field experiments using the PRISM dynamic holography method performed on one spherical shell with imperfections.

ACKNOWLEDGMENTS

The authors are grateful to Dr. Francois Hemez, Los Alamos National Laboratory, and Mr. Isaac Salazar, Graduate Assistant, for supplying the accelerometer modal data they developed earlier.

REFERENCES

1. Baker, W.E., “Axisymmetric Modes of Vibration of Thin Spherical Shell”, ***Journal Acoust Soc Am***; 33:1749-58, 1961.

2. Kalnins, A., “Effect of bending on vibrations of spherical shells”***, J Acoust Soc Am***; 36:74-81, 1964.

3. Wilkinson, J.P., “Natural frequencies of closed spherical shells”***, J Acoust Soc Am***; 38:367-368, 1965.

4. Silbiger, A., “Nonaxisymmetric modes of vibration of thin spherical shells”, ***J Acoust Soc Am***; 34:862, 1962.

5. Niordson, F.I., “Free vibrations of thin elastic spherical shells”, ***Int J Solids Struct***; 20:667-687, 1984.

6. Niordson, F.I., “The spectrum of free vibrations of a thin elastic spherical shell”, ***Int J Solids Struct***; 24: 947-961, 1988.

7. Duffey, T.A. and Romero, C., “Strain growth in spherical explosive chambers subjected to internal blast loading”***, Int. J. Impact Engng***; 28: 967-983, 2003.

8. Jellison, J., Kess, H.R., Adams, D.E. and Nelson, D.C., “Vibration-Based NDE Technique for Identifying Non-Uniformities in Manufactured Parts with Degeneracies”, ***Proceedings of IMECE 2002***, pp. 621-628, New Orleans, LA, Nov. 17-22, 2002.

9. Robertson, A., Hemez, F., Salazar, I. and Duffey, T., ***Modal Testing Repeatability of a Population of Spherical Shells***, LA-14109, Los Alamos National Laboratory, Los Alamos, NM, May 2004.

10. Cloud, G.L., ***Optical Methods of Engineering Analysis***, Cambridge University Press, Ch. 16, pp 360-363, 1998.

11. Pepin, J.E., Thacker, B.H., Rodriguez, E.A. and Riha, D.S., “A Probabilistic Analysis of a Nonlinear Structure Using Random Fields to Quantify Geometric Shape Uncertainty”, 43rd AIAA/ASME/ASCE/AHS/ASC, Structures, Structural Dynamics, and Materials Conference, AIAA 2002-1641, Denver, CO, April 22-25,2002.